place at a real surface in order to minimize surface strain.

Pyridine is seen to have a fortuitous combination of properties which make for an excellent probe of alumina surfaces. Firstly, its low basicity allows for the exclusive observation of Lewis acid sites. Secondly, the sensitivity of the ^{15}N chemical shift for pyridine is sufficient to resolve the different Lewis sites. Finally, the large size (relative to, e.g., NH_3) of the pyridine ring and the conformational restrictions which are imposed upon its constituent atoms allows for the study of the steric properties of the binding site. The site-selective pyridine is seen to be especially informative when used in conjunction with the nonselective ammonia probe molecule,[17] which allows for the study of Brønsted and Lewis acid site distributions on these alumina surfaces.

The present study illustrates how high-field solid-state ^{15}N and ^{2}H NMR spectroscopies can provide new structural insights about the nature of nitrogen Lewis acid/base adducts on γ-alumina surfaces, and possibly the morphology of these surfaces as well. In future work we will examine the possibility of positively identifying each ^{15}N resonance to the appropriate type of cation site by examining a variety of types of aluminas where the cation site occupancy will differ from γ-alumina. If this hypothesis is supported by further experiments, ^{15}N NMR may prove to be a very useful method for determining the distribution of tetrahedral vs. octahedral sites on various alumina surfaces, a number which is difficult to obtain by other methods.

Acknowledgment. The authors wish to acknowledge support from the National Science Foundation via Research Grant CHE 83-06580 and access to the Regional Instrument Facility at the University of South Carolina which is supported by the NSF, Grant CHE 8207445.

Registry No. Al_2O_3, 1344-28-1; pyridine, 110-86-1.

Theoretical Study of the Ammoniated NH_4 Radical and Related Structures

E. Kassab* and E. M. Evleth

Contribution from Dynamique des Interactions Molêculaires, E.R. 271, Tour 22, Universitê Pierre et Marie Curie, 75230 Paris, France. *Received May 19, 1986*

Abstract: The ground- and some of the excited-state surfaces for the reaction of the Rydberg radical NH_4 to give either $NH_3 + H$ or $NH_2 + H_2$ are computed. The preferred ground reaction channel is that observed experimentally, the formation of $NH_3 + H$. The Rydberg character, as well as the low barrier for fragmentation, is rationalized using a Rydberg extended-state structure correlation diagram. The excited-state surfaces show deep potential wells whose forms are also rationalized using this correlation diagram. Calculations on the surface of tetramethylammonium radical show no enhanced stability due to alkyl substitution. Comparative calculations on the complexation energies of $NH_4^+(NH_3)_n$ and $NH_4(NH_3)_n$, $n = 1$–6, show the semiionic character of the Rydberg radical. The variation of stepwise complexation energies with n for the Rydberg species is not completely understood. The stability of solvated NH_4 radical in liquid NH_3 is estimated to be of the same order as $(NH_4^+)_s + (e^-)_s$.

Recently, Gellene, Porter, and co-workers[1] have observed the formation of a series of ammoniated NH_4 radical species, $NH_4(NH_3)_n$, $n = 1, 3$. These species are generated in molecular beams by electron addition to the $NH_4^+(NH_3)_n$ cationic species. The existence of $NH_4(NH_3)_n$ species takes on special interest since the parent radical, NH_4, has not yet been observed in the ground state.[2] Additional interest occurs because this and the H_3 species represent the first characterized members of a broad class of materials referred to as Rydberg radicals. The D_3O radical and the H_3O–water complexed species have also been detected.[3] Although NH_4 was first well characterized by emission,[2a] the existence of mercury amalgams of ammonium and alkylammonium radicals has long been known.[4] The possible condensed-phase existence of ammonium radicals formed by electron capture by ammonium ions is suggested by a number of experimental observations.[5] We have recently proposed[6] the generation of ammoniated NH_4 radicals in the photodecomposition of ammonia and water–ammonia clusters.

If Rydberg radicals exist as complexes or solvated species in the condensed phase, as they do in small clusters, a conceptual problem arises in describing their diffuse electronic structures in the presence of large numbers of other molecules.[7] Even the electronic structure description of the isolated NH_4 species represents a conceptual problem in valence orbital terms. Originally, Mulliken recognized the possible Rydberg character of this radical.[8] Herzberg anticipated[9] the NH_4 radical as a member of

(1) (a) Gellene, G. I.; Porter, R. F. *J. Phys. Chem.* **1984**, *88*, 6680–6684. (b) Jeon, S.; Raksit, J. A. B.; Gellene, G. I.; Porter, R. F. *J. Am. Chem. Soc.* **1985**, *107*, 4129–4133.

(2) (a) Herzberg, G. *Faraday Discuss. Chem. Soc.* **1981**, *71*, 163–173. (b) Whittaker, E. A.; Sullivan, B. J.; Bjorklund, G. C.; Wendt, H. R.; Hunziker, H. J. *J. Chem. Phys.* **1984**, *80*, 961–962.

(3) Gellene, G. I.; Porter, R. F. *J. Chem. Phys.* **1984**, *81*, 5570–5576.

(4) For a review up until 1968, see: (a) Wan, J. K. S. *J. Chem. Educ.* **1968**, *45*, 40–43. Since 1968, see: (b) Kariv-Miller, E.; Nanjundiah, C.; Eaton, J.; Swenson, K. E. *J. Electroanal. Chem.* **1984**, *167*, 141–155. (c) Littlehailes, J. D.; Woodhall, B. J. *Faraday Discuss. Chem. Soc.* **1968**, *45*, 187–192.

(5) (a) Anbar, M. "Solvated Electron", *Adv. Chem. Ser.* **1965**, *No. 50*, 55–81, and references cited therein. (b) Horner, L. "Organic Electrochemistry"; Baizer, M. M., Ed.; Marcel Dekker: New York, 1973; pp 429–443. (c) Brooks, J. M.; Dewald, R. R. *J. Phys. Chem.* **1971**, *75*, 986–987. (d) Brown, O. R. *Electrochemistry* **1974**, *4*, 55–77. (e) Quinn, R. K.; Lagowski, J. J. *J. Phys. Chem.* **1968**, *72*, 1374–1378. (f) Dye, J. L.; DeBacker, M. G.; Dorfman, L. M. *J. Chem. Phys.* **1970**, *52*, 6251–6258. (g) Laitinen, H. A.; Nyman, C. J. *J. Am. Chem. Soc.* **1948**, *70*, 3002–3008. (h) Gedye, R. N.; Sadana, Y. N.; *J. Org. Chem.* **1980**, *45*, 3721–3722 and references cited therein.

(6) (a) Cao, H. Z.; Kassab, E.; Evleth, E. M. *J. Chem. Phys.* **1984**, *81*, 1512. (b) Evleth, E. M.; Cao, H. Z.; Kassab, E. *Photochemistry and Photophysics above 6 eV*; Lahmani, F., Ed.; Elsevier: Amsterdam, 1985; pp 479–495.

(7) (a) For a discussion of high-pressure and condensed-phase effects on Rydberg spectra, see: Robin, M. B. *Higher Excited States of Polyatomic Molecules*; Academic Press: New York, 1974; Vol. I, pp 76–91. (b) Gaathon, A.; Jortner, J. *Can. J. Chem.* **1977**, *55*, 1801. (c) Messing, I.; Raz, B.; Jortner, J. *Chem. Phys.* **1966**, *4*, 4470. (d) Evleth, E. M.; Gleghorn, J. T. *Chem. Phys. Lett.* **1983**, *94*, 373–376.

0002-7863/87/1509-1653$01.50/0

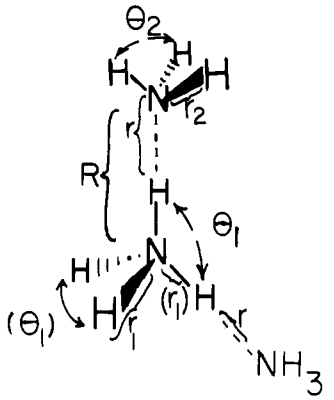

Figure 1. Optimized geometry parameters for the complexes of NH_4 or NH_4^+ with ammonia.

a class of ground-state and excited-state Rydberg radicals generated by the electron binding to filled-shell cationic species. Although earlier theoretical treatments[10] took this possible Rydberg character into account, more recent[11] valence-level MO treatments lead to quantitative predictions that the NH_4 (T_d) structure was not a local minimum on the hypersurface giving NH_3 + H. However, addition of diffuse basis set components yields computations in which the T_d structure is a minimum.[12c,e] The 3s Rydberg character of the ground state of NH_4 and related radicals is now theoretically well established.[12] However, because of the 3s diffuse orbital character of these species, there is a question as to their description in the condensed phase. The conceptual problem of rationalizing the stability of NH_4 and its ammonia complexed forms will be addressed here.

Technical Details

The calculations on the NH_4 radical surfaces used a triple Rydberg (N, 3s,3s′, 3p,3p″; H, 2s) modified Dunning DZ basis (4s2p/2s).[13] Calculation of the ammoniated complexes of NH_4 and $(CH_3)_4N$ reported here used a 4-31G basis set supplemented by a single 3s diffuse orbital on each heavy atom (α_N = 0.020, α_C = 0.015). The SCF calculations were performed using closed- and open-shell RHF and UHF methodologies contained in the program MONSTERGAUSS.[14] The cluster computations RHF radical optimizations were then initiated from the cation MOs and geometries. RHF level geometry optimizations (Figure 1) were carried out using a gradient method with a single negative second-derivative verification for transition-state structures.[14] Two correlation methods were used. MONSTERGAUSS has a single–double CI capability but this is limited to an energy estimation of the lowest state of any particular multiplicity. The excited-state estimations presented here used a correlation method[15] (CIPSI) equivalent to a MRMP2 treatment (multireference Moller–Plesset second order). This method involves first selecting, by an iterative search, a highly interacting CI space (CI coefficient threshold selection used here = 0.02). The correlation energy is then obtained by a second-order perturbation MP treatment of all the configurations in the highly interacting CI space with the excluded space.

Scheme I

$H = H^+ + e^-$	E = +13.6 eV	(1)
$NH_3 + H^+ = NH_4^+$	E = −8.9 eV	(2)
$NH_4^+ + e^- = NH_4$	E = −4.4 eV	(3)
$NH_3 + H = NH_4$	E = +0.3 eV	

Scheme II

$NH_3 + H = NH_3^*$ (n,3s) + H	E = +5.7 eV	(4)
NH_3^* (n,3s) + H = NH_4 (3s)	E = −4.8 eV	(5)
$NH_3 + H = NH_4$	E = +0.9 eV	

The cluster calculations were scaled to the estimated ionization potential of the NH_4 radical (4.73 eV)[16] and NH_3 complexation energy of the NH_4^+ (1.08 eV).[17] Therefore, no zero-point, thermodynamic, or correlation energy corrections were applied to the calculations dealing with the ammoniation. The basis superposition error was investigated in the case of the $NH_4(NH_3)_4$ radical cluster. The purpose of a scaling procedure was to attempt to avoid all these costly corrections so that as large a cluster as possible could be computed at the SCF level.

Results and Discussion

A. Theoretical Characterization of the Stability of the NH_4 Radical. 1. Thermochemical Estimations. In order to rationalize the stabilities of the ammoniated NH_4 radical species we will review some of the qualitative and quantitative reasons for the stability of the NH_4 radical itself. A number of computations[6,10-12] have been generated for this species, but a qualitative rationalization of stability of these kinds of structures still requires clarification.

In Schemes I and II we show two different approximate thermochemical estimations of the reaction energy of the NH_4 radical giving NH_3 + H. Reaction Scheme I uses the known ionization potential (IP) of the hydrogen atom (13.6 eV) and proton affinity of ammonia (8.9 eV),[18] reactions 1 and 2, respectively. In the case of reaction 3, if one assumes a 3s Rydberg electronic structure, $NH_4^+(e^-)_{3s}$ for the NH_4 radical, the IP of the radical should be close to the IP of the lowest excited n,3s Rydberg state of ammonia.[18] In spectroscopic terms, this value is known as the 3s-term value and is measured at 4.4 eV.[18] Based on these figures, the NH_4 is unstable with respect to NH_3 + H by 0.3 eV. However, Gellene and Porter estimated[16] the experimental value of the IP of NH_4 at 4.73 eV. Based on this number, NH_4 and NH_3 + H are about isoergic. Together with tables of Rydberg term values[18] and proton affinities,[19] use of Scheme I permits estimating the thermochemical stabilities of a large number of Rydberg radicals. The combination of large proton affinities and large term values favors the stabilities of Rydberg radicals with respect to fragmentation. Although there are a number of neutral species (e.g., alkylamines) which have larger proton affinities than ammonia, their term values are smaller.[18] The net result is that the NH_4/NH_3 + H system is about the most favorable one with regard to enthalpic stability. However, a large positive entropy is associated with fragmentation, and the general conclusion is that isolated Rydberg radicals are thermodynamically unstable species.[12c,e] The kinetic stability cannot be addressed using Scheme I but will be qualitatively evaluated using Scheme II.

Reaction 4 is the excitation energy of ammonia to its first excited n,3s singlet state. This state can be written in simple electronic structural terms as $(e^-)_{3s}H_3N^+$. Reaction 5 can be viewed as a H atom forming an electron-pair σ bond with the half-filled n orbital on nitrogen. This σ bond is assumed to be the same as for the NH bond in NH_3 (4.8 eV).

$$(e^-)_{3s}H_3N^{+\bullet} + {}^\bullet H = (e^-)_{3s}H_3N^+{:}H$$

(8) Mulliken, R. S. *J. Chem. Phys.* **1933**, *1*, 492.
(9) Herzberg, G. *Electronic Spectra of Polyatomic Molecules*; Van Nostrand: Princeton, NJ, 1966; pp 373–376, 397.
(10) (a) Melton, C. E.; Joy, H. W. *J. Chem. Phys.* **1967**, *46*, 4275–4283. (b) Strehl, W.; Hartman, H. K.; Hensen, B.; Sarholz, W. *Theor. Chim. Acta* **1970**, *18*, 290–308.
(11) (a) Lathan, W. A.; Hehre, W. J.; Curtis, L. A.; Pople, J. A. *J. Am. Chem. Soc.* **1971**, *93*, 6377–6387. (b) Gordon, M. S.; Gano, D. R.; Boatz, J. A. *Ibid.* **1983**, *105*, 5771–5775.
(12) (a) Raynor, S.; Herschbach, D. R. *J. Phys. Chem.* **1982**, *86*, 3592–3598. (b) Broclawik, E.; Mrozek, J.; Smith, V. H., Jr. *Chem. Phys.* **1982**, *66*, 417–423. (c) Cardy, H.; Liotard, D.; Dagelos, A.; Poquet, E. *Ibid.* **1983**, *77*, 287–299. (d) Havriliak, S.; King, H. F. *J. Am. Chem. Soc.* **1983**, *105*, 4–12. (e) Kaspar, J.; Smith, H., Jr.; McMaster, B. N. *Chem. Phys.* **1985**, *96*, 81–95.
(13) Kassab, E.; Gleghorn, J. T.; Evleth, E. M. *Chem. Phys. Lett.* **1980**, *70*, 151–154.
(14) Peterson, M. R.; Poirier, R. A., Department of Chemistry, University of Toronto, Version 1983. For a discussion of the optimization methods in this program, see: Peterson, M. R.; DeMaré, G. R.; Csizmadia, I. G.; Strausz, O. P. THEOCHEM **1983**, *92*, 239 and references cited therein.
(15) (a) Huron, B.; Malrieu, J. P.; Rancurel, O. *J. Chem. Phys.* **1973**, *58*, 5745–5759. (b) For further clarifications, see: Evangelisti, S.; Daudey, J. P.; Malrieu, J. P. *Ibid.* **1983**, *75*, 91–101.
(16) Gellene, G. I.; Cleary, D. A.; Porter, R. F. *J. Chem. Phys.* **1982**, *77*, 3471–3477.
(17) (a) Meot-Ner, M. *J. Am. Chem. Soc.* **1984**, *106*, 1257–1264. (b) Meot-Ner, M. *Ibid.* **1984**, *106*, 1265–1272 and references cited therein.
(18) Reference 7a, Vol. I, pp 208–229.
(19) Bartness, J.; Scott, E.; McIver, R. T., Jr. *J. Am. Chem. Soc.* **1979**, *101*, 6064–6056.

Table I. Computation of the Ground State of the NH_4 Radical at Three Points along the Potential Surface for NH Bond Rupture

structure	$R(N-H_r)$ (Å)	RHF energy[a] (au)	Rydberg[b] occ	correlation energy CISD[c]	C_0[d]	CISD + corr	CIPSI (MRMP2)[f]
NH_4 (T_d)	1.033	−56.663 70	1.08	−0.131 96	0.973	−0.139 01	−0.137 82
NH_4 (C_{3v}, TS)	1.369[g]	−56.639 68	0.57	−0.131 69	0.968	−0.144 21	−0.142 92
NH_4 (C_{3v})	4.000[h]	−56.672 15[i]	0.23	−0.121 26	0.975	−0.127 16	−0.127 08
NH_3 (C_{3v})		−56.172 83[i]					−0.127 08
H		−0.499 34					

[a] Rydberg modified Dunning basis; see text for description. [b] Total electron population in Rydberg space. [c] Frozen core, single and double CI, 76 configurations. [d] Main CI coefficient. [e] Davidson correction = $(1 - C_0)^2 E_{CISD}$. [f] See text for description of method. CI diagonalization of all configurations (ca. 17) having interaction mixing coefficients greater than 0.02 + MP2 treatment of between 300 000 and 360 000 determinates. [g] TS, RHF transition-state optimization, one negative value for Hessian matrix; other optimized parameters are $R(NH)$ = 1.018 Å, $\angle H_rN-H$ = 107.4°. [h] $R(NH)$ = 1.007 Å, $\angle H_rN-H$ = 103°. [i] The sum of the RHF energies of H + NH_3 = −56.672 17 au for $R(NH)$ = 1.007 Å, $\angle L_rN-H$ = 103°; L_r = lone pair.

Table II. CIPSI Level Excitation Energies for the NH_4 Radical along the NH Bond Rupture Coordinate

structure	$R(N-H_r)$ Å	relative energies (eV) ground state (1^2A_1,3s)	excited states $2^2A_1(3p_z)$	$1^2E(3p_{x,y})$	$3^2A_1(4s_z)$	$2^2E(4p_{x,y})$
NH_4 (T_d)	1.033	0.00[a]	1.66	1.66	2.65	NC
NH_3–H (C_{3v})	1.250	0.34	2.09	2.28	2.99	3.59
NH_3–H (C_{3v})	1.369	0.52	2.46	2.83	3.37	4.14
NH_3–H (C_{3v})	2.000	0.23	3.90	5.11	5.66	6.45
NH_3–H (C_{3v})	2.500	0.13	4.30	5.72	5.00	5.89
NH_3–H (C_{3v})	3.000	0.09	4.64	6.15	4.83	6.19

[a] Zero reference energy = −56.8012 au, the sum of the RHF + CIPSI energy from Table I. State symmetries given for C_{3v} point group; z axis is the reaction pathway.

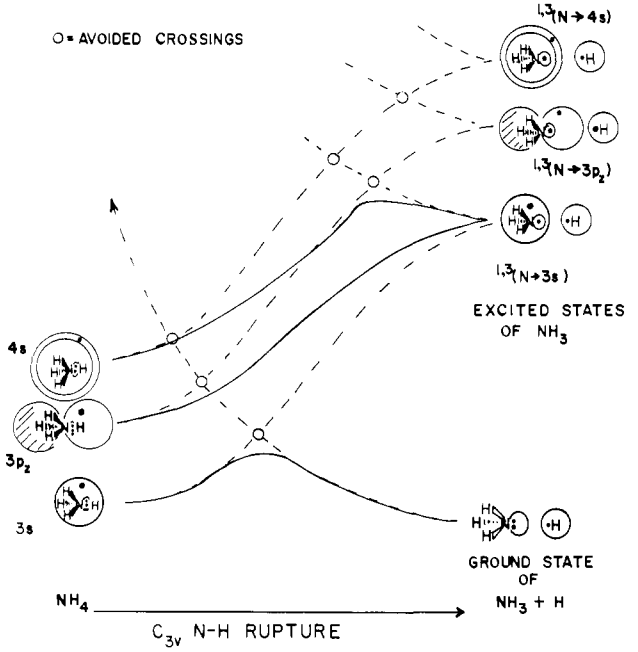

Figure 2. Structural correlation diagram for the $^2A_1$ symmetry ground- and excited-state correlations of the lower states of the NH_4 radical with NH_3 + H. The large orbitals represent 3s, 3p, and 4s Rydbergs.

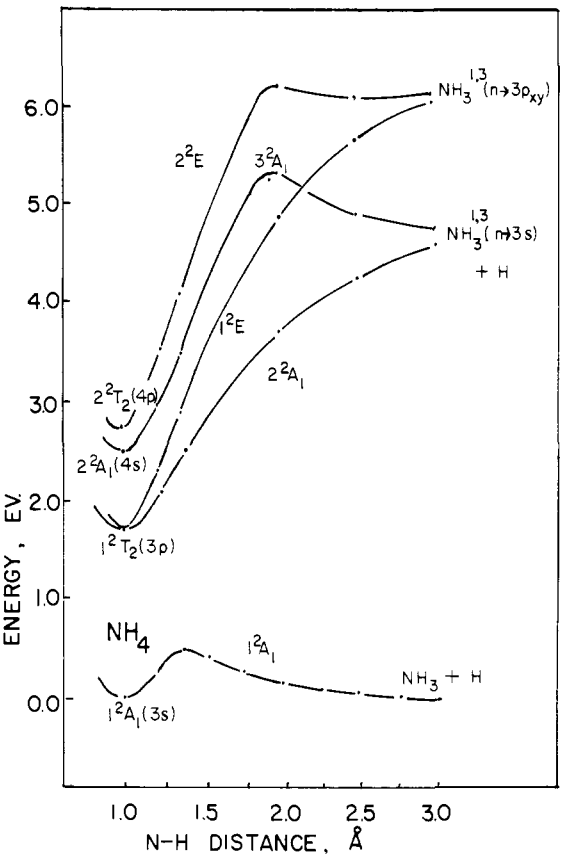

Figure 3. MO–CIPSI computed surfaces for the ground and lower excited states of the NH_4 radical with NH_3 + H. See Table II for details of the computations and zero reference energy.

The state-to-state correlation diagram (Figure 2) using this kind of electronic structural analysis is more complicated than Scheme II indicates. First of all, the singlet–triplet splitting in even-electron Rydberg species is small, and the state-to-state correlations for an overall doublet species are complicated at the large separation limit where the species have three open shells. The dotted lines in Figure 2 show the natural[20] or structurally intended[21] correlations having $^2A_1$ symmetry. However, avoided crossings occur and the real state-to-state correlations are shown by solid lines. Because of the loss of Rydberg character occurring along the ground-state surface, there are changes in Rydberg character occurring along the excited-state surfaces. Although Scheme II predicts that NH_4 is more unstable (0.9 eV) than Scheme I, Figure 2 does yield the qualitative prediction that it should have 3s Rydberg character. More importantly, the ground-state surface is anticipated to have an avoided crossing energy barrier interconnecting the NH_4 (T_d) structure with the NH_3 + H fragments.

(20) Devaquet, A.; Sevin, A.; Bigot, B. *J. Am. Chem. Soc.* **1978**, *100*, 2009–2012.
(21) Evleth, E. M.; Kassab, E. *Theor. Chim. Acta* **1982**, *60*, 385.

Additional analysis of the excited-state features of Figure 2 will be discussed below.

2. Computations. Computations of the critical points along the ground-state NH bond rupture surface are shown in Table I. Table II shows the relative energies for some of the excited-state surfaces, this being also shown in Figure 3. The kinetic implication of the theoretical barrier found for the ground-state surface has already been analyzed.[12c,e] Therefore, we will concentrate here on the new features that these computations produce.

a. Ground-State Surface for the $NH_4 = NH_3 + H$ Fragmentation. The main qualitative feature of interest in Table I is that the transition state along the ground-state surface has the anticipated valence/Rydberg character (ca. 40/60). The ground-state NH_4 (T_d) structure has about one electron (1.08) in diffuse orbital space. This justifies the qualitative view that the ground state of this species is described as an electron in a 3s orbital bound to a NH_4^+ core. The residual diffuse orbital (0.23) component seen at 4.0 Å N–H distance is not essentially Rydberg-like but extended valence in character and demonstrates that the Mulliken population should only be used semiquantitatively.[13] More seriously, what appears not to be in agreement with Figure 3 is that the ground-state CI wave function is essentially monoconfigurational along all points of the surface ($C_0 \simeq 0.97$).[22] However, it can be demonstrated from orbital correlation diagrams[23] that in this case the Rydberg loss occurs at the SCF level.[24] Figure 2 is configurationally valid at the non-SCFCI level.[21]

Our energy barrier (12 kcal/mol) and ergicity of this decomposition (2 kcal/mol) can be corrected to 5 and −7, respectively, using the zero-point energy corrections of Cardy et al.[12c] However, the highest level of theoretical treatment[12e] (SDCI/TZP+3s,p) shows NH_4 and NH_3 + H isoergic for the vibrationless ground state with approximately the same barrier. This barrier energy is so low that tunneling plays an important role in determining the stability of the NH_4 species.[1-3,12c,e] The lifetimes of related ammonium radicals should also be increased by alkyl substitution.[1,3] We will return to the case of alkyl-substituted species later.

b. Excited-State Surfaces. Figure 3 shows a comparison of the ground- and excited-state surfaces for the $NH_4 = NH_3 + H$ fragmentation which confirms the expectations of the state–state correlation diagram (Figure 2). The surface behaviors shown in Figure 3 demonstrate that excited molecular Rydberg–atom interactions can be highly bonding if a favorable situation exists. In the case of NH_4, all the excited states shown are adiabatically stable with regard to N–H fragmentation channels. The nonadiabatic vibronic coupling influencing excited-state stabilities has been discussed by Raynor and Herschbach.[12a] The energies shown in Figure 3 are not quantitatively accurate since at the N–H large distance limit the 3^2A_1 surface should approach the 5.7-eV excitation energy of the n,3s singlet state of NH_3.[18] In addition, because of the photochemical instability of the first excited state of NH_3, one has difficulty imagining an experiment in which atomic hydrogen interacts with excited NH_3. A final point to note in Figure 3 is that the 3^2A_1 and 2^2E doublet surfaces display the barrier behaviors anticipated from the avoided crossing correlations shown in Figure 2.

c. Ground- and Excited-State Surfaces for the $NH_4 = NH_2 + H_2$ Fragmentation. Cardy et al.[12c] have also analyzed the ground-state channel for the NH_4 giving $NH_2 + H_2$. We show the computed ground- and a two excited-state surface behaviors under C_{2v} symmetry constraints in Figure 4. Under C_{2v} symmetry restraint, the ground state of NH_4 correlates with H_2 and the first excited state of NH_2. As viewed from the product side, all surfaces are Rydbergizing as H_2 approaches the three valence states of NH_2. A similar structural state-to-state correlation diagram as shown in Figure 2 can also be constructed for the $NH_2 + H_2$ system which anticipates the surface behavior computed in Figure 4. The ground- and excited-state crossing shown in Figure 4 will be avoided on distortion from C_{2v} symmetry. A technically interesting feature of the $^2A_1$ surface is that at the RHF level the H_2 departure from NH_4 is accompanied by a progressive increase in the HH distance along the optimized surface. However, as in the case of Cardy et al.[12c] we were unable to obtain a C_{2v} restrained transition state. As a consequence, the geometry parameters shown in Figure 4 in the region of the $^2A_1$ transition state were chosen from a series of after-CIPSI correlation estimates. A linear geometry scan was then imposed in which the HH bond distance was linearly decreased in passing from NH_4 to $NH_2 + H_2$ through the after-CI-optimized $^2A_1$ transition state. Although this procedure may be deceptive, it leads to the qualitative conclusion that the ground-state barrier remains larger for H_2 departure from NH_4 than for simple H fragmentation. The C_{2v} $^2B_1$ surface proved to be mainly biconfigurational in the region of the maximum shown in Figure 4. Any symmetry breaking of the system would likely produce increased repulsion between the ground and first excited surfaces and probably not lower the excited-state barrier. Therefore, it is concluded that for the H_2 fragmentation channel the lower excited states of NH_4 will be adiabatically stable for several electron volts.

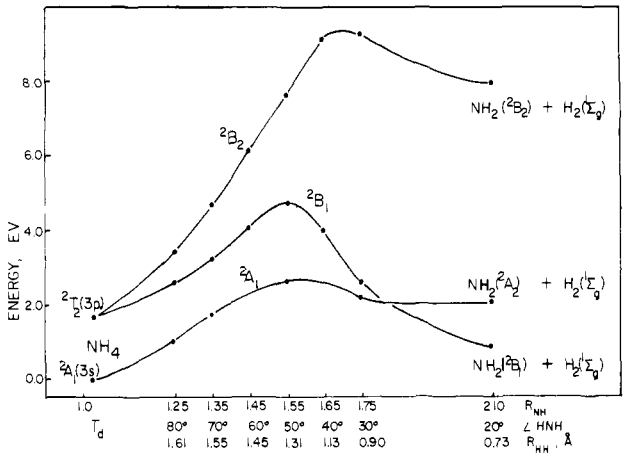

Figure 4. MO–CIPSI ground- and lower excited-state surfaces for NH_4 radical giving NH_2 + H. The zero energy is same as shown in Table II.

d. The Ground-State Stability of Alkylammonium Radicals. The preparation of a large number of mercury amalgams of alkylammonium radicals is reported.[4] Although unstable at room temperature, the decomposition of these materials is considerably slowed below 0 °C.[4] Gellene and Porter also observed that in the gas-phase fragmentation of the CH_3NH_3 radical, N–H bond rupture dominates C–N rupture.[1b,3] The stability of C–N bonds is also encountered in the absorption threshold of trialkylamines.[25] In a previous study,[23] we estimated that the activation energy for C–N bond rupture in excited methylamine is about 1 eV above the zero vibrational level of the n,3s state. Our hyperconjugative rationalization[23] of the relative stability of C–N over N–H bonds in n,3s excited species should not be applicable for a tetrahedral species. The C–N bond rupture surface scan for the $(CH_3)_4N$ species (Figure 5) showed an RHF barrier, 13 kcal/mol, less than the RHF barrier, 15 kcal/mol, for the N–H rupture in NH_4 (Table I). Since geometry optimization, correlation, and zero-point energy correction will reduce further the barrier for C–N rupture, our qualitative conclusion is that fully alkylammonium radicals are unstable species whose activation energies for decomposition are not in excess of about 10 kcal/mol. Therefore, the room-temperature half-lives of such species would fall in the milli- to microsecond region. The relative stabilities of alkylammonium mercury amalgams are due to some factor other than the intrinsic stabilities of the alkylammonium radicals.

(22) The SDCI (with Davidson correction) and CIPSI method give approximately the same correlation energy. The CIPSI method is more cost efficient by a factor of 2 in terms of machine time, but more labor intensive (not a black box method).

(23) Kassab, E.; Gleghorn, J. T.; Evleth, E. M. *J. Am. Chem. Soc.* **1983**, *105*, 1746–1753.

(24) Mulliken, R. S. *Acc. Chem. Res.* **1976**, *9*, 7–12.

(25) (a) Cureton, C. G.; Hara, K.; O'Connor, D. S.; Phillips, D. *Chem. Phys.* **1981**, *63*, 31–49 and references cited therein. (b) Matsumi, Y.; Obi, K. *Ibid.* **1980**, *49*, 87–93.

Table III. Energies and Structures of the Monomers NH_4^+, NH_3 and Cationic Complexes, $NH_4^+(NH)_n$

species	sym	energy[a] au	optimized geometrical parameters[b] R	r	r_1 (r_1)	θ_1 (θ_1)	r_2	θ_2
NH_4^+	T_d	−56.4594			1.012			
NH_3	C_{3v}	−56.1070					0.991	115.6
$NH_4^+(NH_3)$	C_{3v}	−112.6143	2.732	1.647	1.008 (1.085)	109.7	1.004	109.4
NH_3–H–NH_3^+	D_{3d}	−112.6127[c]	2.594	1.297	1.006	110.0		
$NH_4^+(NH_3)_2$	C_{2v}	−168.7579	2.828	1.777	1.006 (1.051)	108.9 (110.4)	1.002	110.0
$NH_4^+(NH_3)_3$	C_{3v}	−224.8947	2.902	1.860	1.005 (1.036)	110.0	1.001	110.6
$NH_4^+(NH_3)_4$	C_{3v}	−281.0271[d]	2.967	1.940	1.027	109.5	1.000	111.1
$NH_4^+(NH_3)_5$	C_s	−337.1478	same internal geometries as $n = 4$, external					
$NH_4^+(NH_3)_6$	C_s	−393.2684	NH_3 molecules have H–NH_3 bond distances of 2.37 Å with linear N–H–N bonds					

[a] RHF/4-31G+3S level. [b] See Figure 1 for geometry specifications. [c] Transition state for proton transfer. [d] The SCF energy of NH_3 in the presence of the phantom orbitals of NH_4 plus $3NH_3$ at this geometry is −56.1093 au. The SCF energy of NH_4^+ in the phantom orbitals of $4NH_3$ is −56.4603 au. The total fragment energies under phantom conditions is −280.8976 au.

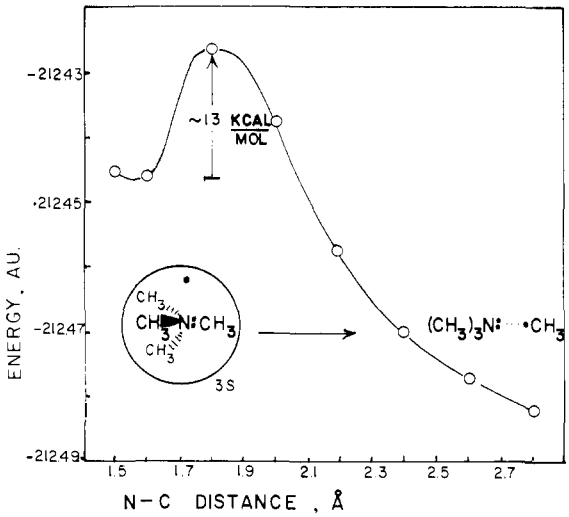

Figure 5. 4-31G+3S_c, 3S_n RHF scan of the N–CH_3 bond rupture of the tetramethylammonium radical to give trimethylamine plus a methyl radical. The geometry elements kept constant are C–N, 1.474; C–H, 1.081; NCH, 105°; T_d to C_{3v} symmetry restraint; initial T_d energy, −212.445 96 au. See text for an estimate of the lowering of the RHF barrier, 13 kcal/mol, with correlation.

B. Characterization of the Stability of Complexed NH_4 Radicals. 1. Qualitative Analysis. The above calculations lead to the conclusion that long-lived ground-state Rydberg radicals will be found only under special conditions. Mercury amalgam complexation of ammonium radicals may fall into a special class in which the system undergoes Rydberg loss by electron delocalization (injection) into the metal. This supposition emphasizes the metallic nature and reductive chemical properties of Rydberg radicals[4b] and suggests a number of complexation possibilities. Polar molecule complexation provides one of the simplest methods of stabilization of Rydberg radicals. The study presented below characterizes this kind of Rydberg radical stabilization.

The problem of how complexation will alter the Rydberg character of a Rydberg species is not completely clear. In the case of the NH_4 radical, its $(e^-)_{3s}$,NH_4^+ character leads to the qualitative expectation that the complexation of this species with polar molecules will be strongly quadrupole–dipole in character. This should lead to complexation energies stronger than for NH_3–NH_3 (ca. 0.10 eV)[26] but weaker than for the ion–molecule interaction, NH_4^+ with NH_3 (1.08 eV).[17] Our previous large basis set estimate[6a] of the NH_4/NH_3 complexation energy (0.38 eV) fell in this region.

Table IV. Complexation Energies for the Reactions

(i) $NH_4^+ + nNH_3 = NH_4^+(NH_3)_n$ $E_{n,0}$

(ii) $NH_4^+(NH_3)_{n-1} + NH_3 = NH_4^+(NH_3)_n$ $E_{n,n-1}$

species[a]	complexation energies $E_{n,0}$	$E_{n,n-1}$	$E_{n,n-1}$ scaled[b]	$E_{n,n-1}$ exptl[c]
$NH_4^+(NH_3)$	1.30	1.30	1.08	1.08
$NH_4^+(NH_3)_2$	2.30	1.00	0.83	0.76
$NH_4^+(NH_3)_3$	3.11	0.81	0.67	0.60
$NH_4^+(NH_3)_4$	3.80[d]	0.69	0.59	0.54
$NH_4^+(NH_3)_5$	4.17	0.37	0.30	0.41
$NH_4^+(NH_3)_6$	4.54	0.37	0.30	

[a] Values computed from energies shown in Table III. [b] All values scaled by 1.08/1.30 = 0.83. [c] Reference 18. [d] 3.53 eV using a basis set superposition error correction computed from energies shown in the footnote of Table III. This can be compared to 3.17 eV for the sum of the scaled values and 2.98 eV experimentally.

With regard to the nearly isoergic $NH_4 = NH_3 + H$ reaction channel, any significant extra complexation energy of NH_4 with NH_3 over that of NH_3 with itself (presuming that H atom has a negligible complexation energy with NH_3) will retard the thermal fragmentation of $NH_4(NH_3)_n$ clusters along the channel:

$$NH_4(NH_3)_n = (NH_3)_{n+1} + H$$

Tunneling will not play a role if the reaction is endoergic.

2. Comparative Stabilization Energies for the Ammoniation of NH_4^+ and NH_4. a. Complexation Energies of NH_4^+. Table III contains the energies and optimized geometrical parameters for the complexes $NH_4^+(NH_3)_n$ for $n = 1, 4$. The energies shown for the complexes $n = 5$ and 6 are not for optimized structures. In these latter two cases, the internal $NH_4^+(NH_3)_4$ structure is assumed from the calculation on that structure. Subsequently, the first and second additional NH_3 units are added to different internal NH_3 groups of the first solvation shell. Linear N–H--NH_3 bond and H--N bond distances (2.37 Å) are assumed. The latter is taken from an optimized C_s structure of the NH_3 dimer.[26]

The complexation energies computed from the energies shown in Table III are shown in Table IV. Experimental determinations of the individual stepwise complexation energies of this system are probably accurate to within 0.05–0.1 eV. First of all, the computed complexation energy for $n = 1$, 1.30 eV, is not in good agreement with the experimental value of 1.08 eV.[17] Accurate theoretical estimates of ion–molecule complexation energies require using larger basis sets than employed here, plus zero-point, thermodynamic, correlation,[26] and basis-set superposition error corrections.[27] In addition, a fully consistent analysis would require computing the low-energy frequencies outside the harmonic ap-

(26) (a) Frisch, M. J.; Pople, J. A.; Del Bene, J. E. *J. Phys. Chem.* **1985**, *89*, 3664–3669. (b) Del Bene, J. E.; Frisch, M. J.; Pople, J. A. *Ibid.* **1985**, *89*, 3669–3674.

(27) Latajka, Z.; Scheiner, S. *Chem. Phys. Lett.* **1984**, *105*, 435–439.

Table V. Structures of the Monomers NH_4, NH_3, and the Radical Complexes $NH_4(NH_3)_n$ for n = 1–6

		optimized geometrical parameters[a]						
species	sym	energy	R	r	r_1 (r_1)	θ_1 (θ_1)	r_2	θ_2
NH_4	T_d	−56.6064[b]			1.019			109.5
NH_4	T_d	−56.6065[c]			1.019			109.5
NH_3	C_{3v}	−56.1070[b]					0.991	115.6
$NH_4(NH_3)$	C_{3v}	−112.7321[b]	2.828	1.780	1.015 (1.048)	108.9	1.000	111.8
$NH_4(NH_3)$	C_{3v}	−112.7323[c]	2.828	1.780	1.016 (1.048)	108.9	1.000	111.8
$NH_4(NH_3)$[d]	D_{3d}	−112.7241[c]	2.576	1.288	1.008	109.7		
$NH_4(NH_3)_2$	C_{2v}	−168.8533[b]	2.855	1.814	1.011 (1.041)	108.8 (110.9)	1.000	112.0
$NH_4(NH_3)_3$	C_{3v}	−224.9752[b]	2.884	1.849	1.006 (1.035)	109.8	1.001	111.8
$NH_4(NH_3)_4$	C_{3v}	−281.1010[b]	2.946	1.919	1.027	109.5	1.000	111.7
$NH_4(NH_3)_5$	C_s	−337.2168[b]	same internal geometries as n = 4, external					
$NH_4(NH_3)_6$	C_s	−393.3328[b]	NH_3 molecules have H–NH_3 bond distances of 2.37 Å with linear N–H–N bonds					

[a] See Figure 1 for geometry specifications. [b] RHF/4-31G+3S. [c] UHF/4-31G+3S. [d] Transition state for hydrogen transfer, H_3N--H--NH_3. All other structures are complexes between NH_4 and NH_3. [e] The energy of NH_4 in the phantoms of $4NH_3$ is −56.6084 au. Using the NH_3 value for a phantom orbital calculation shown in Table III, the total RHF energy of the fragments under phantom conditions is −281.045 68 au.

Table VI. Adiabatic IP and Complexation Energies for the Reactions

(i) $NH_4 + nNH_3 = NH_4(NH_3)_n \quad E_{n,0}$

(ii) $NH_4(NH_3)_{n-1} + NH_3 = NH_4(NH_3)_n \quad E_{n,n-1}$

	adiabatic IP, eV		complexation energies, eV		
species[a]	IP calcd	IP scaled[b]	$E_{n,0}$	$E_{n,n-1}$	$E_{n,n-1}$ scaled[c]
NH_4	4.00	4.73[b]			
$NH_4(NH_3)$	3.21	4.07	0.51	0.51	0.42
$NH_4(NH_3)_2$	2.60	3.56	0.90	0.39	0.32
$NH_4(NH_3)_3$	2.19	3.22	1.30	0.40	0.33
$NH_4(NH_3)_4$	2.01	3.05	1.81[d]	0.51	0.42
$NH_4(NH_3)_5$	1.88	2.85	2.05	0.24	0.20
$NH_4(NH_3)_6$	1.75	2.65	2.29	0.24	0.20

[a] Values computed from energies shown in Table V. [b] IP scaled from the known IP for n = 0, 4.73 eV (ref 1 and 3) and the scaled complexation energies for the cation (Table IV) and the radical (this table); see Figure 7 for visual representations. [c] Scaled using same factor (0.83) as used in Table IV. [d] 1.51 eV using a basis set superposition correction computed from the energy shown in the footnote of Table V. The sum of the scaled value is 1.50 eV.

proximation.[28] Since these technically preferred procedures are not financially feasible for large systems, we have opted to use the known complexation energy for n = 1 to scale the other computed complexation energies for *both* the cation and radical clusters. These scaled values were obtained by multiplying the theoretical complexation energies by 1.08/1.30. As shown in Table IV, this scaling procedure produces stepwise cation complexation energies that are within about 0.1 eV of the experimental values for n = 2–5. We tested the role of the superposition error for n = 4 (footnotes of Tables III and IV). The total unscaled complexation energy is reduced from 3.80 to 3.53 eV on correction for the superposition error. This corrected value still does not approach the experimental value of 2.98 eV. The scaled value of 3.17 eV already compares reasonably with the experimental value. Any major improvement in the complexation energies would require a basis set having polarization functions. In addition, the intrinsic problems[29] surrounding the issue of the basis set superposition error make it unlikely that the energies of systems of the size treated here can be adequately adjusted even if a larger basis set were employed.

(28) Del Bene, J. E.; Mettee, H. D.; Frisch, M. J.; Luke, B. T.; Pople, J. A. *J. Phys. Chem.* **1983**, *87*, 3279–3282. This will be especially true for hindered rotor and low-barrier double-well potentials.

(29) (a) Schwenke, D. W.; Truhlar, D. G. *J. Chem. Phys.* **1985**, *82*, 2418–2426. (b) Davidson, E. R.; Feller, D. *Chem. Rev.* **1986**, *86*, 681–696.

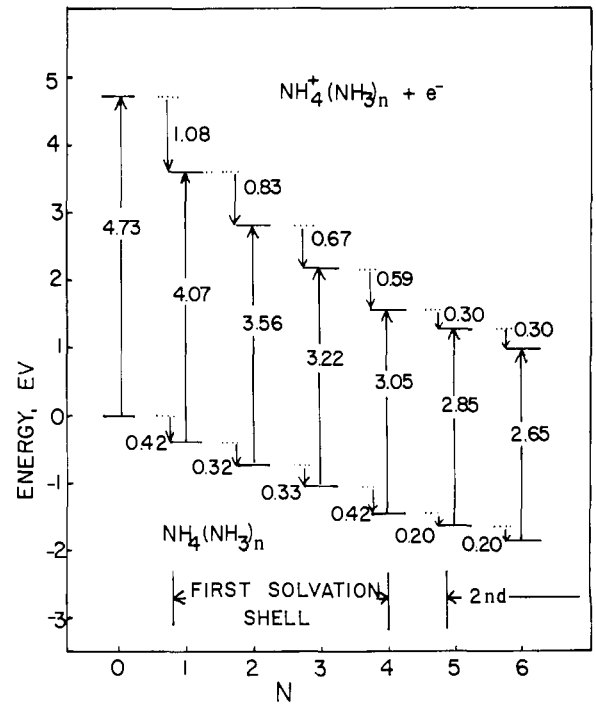

Figure 6. Scaled complexation energies and ionization potentials for the ammoniated NH_4^+ ion and NH_4 radical. See text for explanation of scaling procedure using the ionization potential of NH_4 radical and complexation energy of NH_4^+ with NH_3 as references.

b. Complexation Energies of the NH_4 Radical. Calculations on the $NH_4(NH_3)_n$ complexes are shown in Table V. Most of these calculations were computed at the RHF level with a few comparative computations on the UHF level. Since these radical species are 3s Rydberg in character, little energy difference is encountered using these two different methodologies. The RHF procedure was preferred here since the initiation of the radical computations could be done using the MOs of the closed-shell cation. For the very large computations, n = 5 and 6, the cation MOs and taped stored integrals allowed us to realize the calculations on the radical species at a reasonable price without attempting to obtain the disk storage on the CPU system.

Using these scaled stepwise complexation energies and the measured IP of NH_4 (4.73 eV),[3] the other IPs for n = 2–6 were computed. The details of these computations are shown in Table VI, and the relative complexation behavior of the cation and radical clusters is shown visually in Figure 6. We note that the same kind of scaling procedure allowed an accurate theoretical

estimation for the IP of NH_4 (4.66 eV). The $n = 1$ scaled complexation energy shown in Table VI, 0.42 eV, is close to our previous larger basis set estimate of 0.38 eV.[6a]

The stepwise complexation energies of the cation complexes diminish in a regular fashion. Moet-Ner[17b] pointed out that this behavior is general in a large number of ion–molecule complexation energies. The stepwise complexation energies for the radical complexes do not show the same behavior. This lack of regularity in the stepwise complexation energies of these species indicate some structural complications which are explored below.

c. Comparative Structural Analysis. The NH_4^+ clusters are ion–molecule species whose complexation energies are rationalizable[30] on the basis of charge–dipole, charge–polarizibility interaction potentials. As the size of ion–molecule cluster increases, charge dispersion and dielectric shielding will generate a progressive decrease in the stepwise complexation energies. In the case of the $NH_4^+(NH_3)_n$ clusters, a critical geometrical parameter is the N–N distance (R) shown in Table III. This distance increases regularly from 2.73 to 2.97 Å as n goes from 1 to 4. At the same time, the average unscaled complexation energy per NH_3 group falls from 1.30 to 0.95 eV. A plot of this complexation energy per group vs. R is linear, similar to energy–structures relationships found in hydrogen-bonded ion–molecule complexes.[31] The radical clusters do not behave in this manner. In these species the value of R does increase but not in a regular fashion. There is a large increase from $n = 3$ to $n = 4$. The unscaled complexation energy per NH_3 group varies between 0.51 to 0.43 eV for n = 1–3, but rises to 0.45 eV at $n = 4$. Our precomputational assumption had been that in all cases the radical clusters would have larger N–N distances than the corresponding cation clusters. This assumption was based on the idea that an ion–molecule complex will always be more tightly bound than a corresponding, structurally similar, neutral species. Rydberg radical complexes species have an added complication with regard to the Rydberg electron. Some sort of bubble effect is anticipated[7] in which empty space has to be retained for the Rydberg electron. Any incursion into this space is resisted. Within this context we anticipated that the NN distance in the $n = 4$ radical cluster would be larger than for the corresponding cation. In fact, this distance was smaller, 2.946 Å, than for the cation, 2.967 Å. We will attempt to clarify why this does not occur by examining the electron distribution in these materials.

d. Rydberg Character of the $NH_4(NH_3)_n$ Clusters. Mulliken population analyses show nearly the same net atomic charge on the complexed H atom of the central NH_4^+ ion for *both* the cation and radical species (0.51–0.56). The charge on the uncomplexed H atom in NH_4^+ is of the order of 0.41–0.49 while the charges on the H atom of the NH_3 complexing units are lower, 0.33–0.38. Therefore, within the context of atomic charge on the H atoms, the internal valence structures of the cation and radical species are similar.

With regard to the location of the Rydberg electron in the radical cluster species, we show the nitrogen spin densities in Figure 7. For the most part, these densities reflect the importance of the 3s Rydberg component on each N atom. Except for the case of the transition state (TS) for hydrogen transfer, which we will discuss below, all spin densities are obtained using the RHF method. Exploitation of Figure 7 requires special explanation. Conceptually speaking, RHF spin densities can only be positive. The negative RHF 3s spin densities shown in Figure 7 are artifacts of the Mulliken population analysis at the Rydberg level.[13] Conceptual use of these spin populations has to be made with reference to the fact that the total spin = 1. In particular, the large size of a 3s MO means that a number of different base orbital combinations can be used to obtain the same overall electron density distribution of this orbital. In the case of the uncomplexed NH_4 radical a nitrogen-centered 3s orbital yields a species having

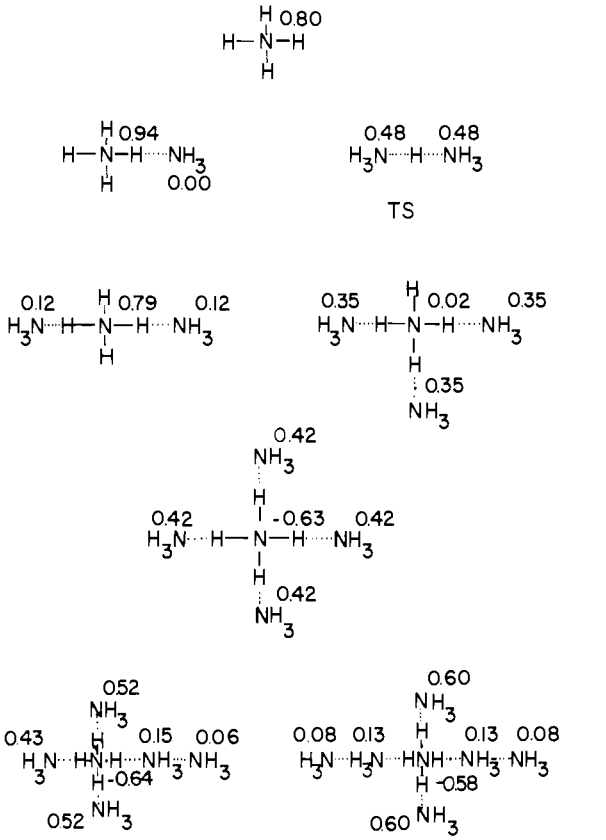

Figure 7. RHF spin nitrogen spin densities in the NH_4 complexes. These spin densities are mostly 3s in character. See text for a discussion of the redistribution of this space on substitution of NH_3 units.

a UHF energy of −56.6065 au (Table V). Suppressing this 3s orbital and placing four 3s orbitals originating from each H atom produces a species having an energy of −56.6047 au with a total spin density (0.84) computationally associated with the H atoms. However, the two different 3s orbital descriptions are qualitatively the same. The second description uses an redundant 3s basis having four components. Optimizing the positions (and exponents) of the four phantom 3s orbitals would eventually produce a better energy than the case of one system centered 3s orbital.

As seen by examining Figure 7 the central nitrogen of the NH_4 unit dominates the spin density for $n = 0$–2. At $n = 3$, the spin densities are transferred to the external N atoms of the complexing NH_3 groups. This is maintained at $n = 4$ with the central N atom supporting a high negative spin density. For $n = 5$ and 6, in which the external NH_3 groups themselves are further complexed by other NH_3 groups, the spin densities are forced off these NH_3 units to increase the densities on the uncomplexed NH_3 units. The major question that occurs is whether the spin densities on the external NH_3 units in the $NH_4(NH_3)_4$ cluster are due to an advantageous use of the 3s components of the NH_3 units or are required because the NH_3 units occupy space which was empty in the case of uncomplexed NH_4. The basis set superposition calculation, in which the NH_4 radical is computed in the phantoms of $4NH_3$, produced (footnote, Table V) an energy lowering of only 0.05 eV. The spin density is associated with the NH_4 3s orbital (0.882), not with the phantom nitrogens (−0.015 each). The use of the 3s orbitals on the external real NH_3 units appears required because they occupy the 3s space of the NH_4 unit. The energetic consequences of this are not completely clear, but it is not serious at the $n = 4$ radical cluster level nor does it manifest itself at the $n = 5$ and 6 level. We were unable to technically carry out the calculations at a $n > 6$ level that might show a bubble effect in this system. In any case, we have no explanation for the lack of regularity in the stepwise complexation energies of the radical clusters.

e. Estimations of the Stability of the NH_4 Radical in Liquid NH_3. Based on other work in this laboratory[32] on bubble-state

(30) Su, T.; Bowers, M. T. *Gas Phase Ion Chemistry*; Bowers, M. T., Ed.; Academic Press: New York, 1979; Vol. 1, pp 84–117.
(31) Cao, H. Z.; Allavena, M.; Tapia, O.; Evleth, E. M. *J. Phys. Chem.* **1985**, *89*, 1581–1592.

structures, the Rydberg electron will avoid the valence electron space and create or seek empty electron space. In condensed media, the best analogy is that of a bubble which, if constraints are made on its natural size in a particular direction, will bulge somewhere else. In the case of NH_3–H_2 and NH_3–He clusters,[32] the systems are unstable in their n,3s excited states for vertical excitations from optimized ground-state geometries. An excited-state bubble is created by repulsion of the H_2 or He units to distances in excess of 5 Å. However, in the case of excited NH_3 clusters,[6a,b] an exoergic valence ion–molecule reaction channel first leads the system to generate complexed (NH_4, NH_2) radicals pairs. Therefore, in this case or the case treated here, the condensed-phase problem involves treating the bubble states in NH_4 clusters.

In the case of the Rydberg radical clusters, there is sufficient available Rydberg orbital space for $n = 1$ and 2 near the NH_4^+ core. For $n = 3$–6, more remote space is selected by using the 3s orbitals associated with the unperturbed NH_3 groups. Where most of the Rydberg electron is located cannot be determined without computing the integrated electron density. In excited NH_3, the maximum for the 3s electron density lies immediately exterior to the H atoms.[24] We assume that for $NH_4(NH_3)_4$ the maximum 3s density will be immediately exterior to the H atoms of the complexing NH_3 units. This also means that the region between the complexing NH_3 units is also available. However, the $n = 5$ and 6 computations indicate the Rydberg use of this region is perturbable. Owing to the necessity of maintaining free Rydberg space, full solvation around the $NH_4(NH_3)_4$ unit may not produce the further lowering of the total complexation energy indicated by the $n = 5$ and 6 computations. In condensed media, the mainly Coulombic binding of an electron in a Rydberg orbital to a cationic core requires close orbital-core proximity. The binding of the electron with the solvent itself is weak and not observed for ammonia clusters with n below 35.[33] However, for liquid ammonia the solvation energy is estimated at 0.99 eV.[34] Given all these factors we now make an estimate for the enthalpy for reactions 6 and 7 in liquid NH_3.

$$(NH_4)_s = (NH_3)_s + (H)_s \quad (6)$$

$$(NH_4)_s = (NH_4^+)_s + (e^-)_s \quad (7)$$

The bubble speculation leads to the expectation that the stepwise NH_4 complexation energies would tend to zero and perhaps become destabilizing as the radical cluster size increases. This expected result may not be computationally encountered until the cluster size exceeds the level treated here, e.g., $n > 7$. Several possible situations can be envisaged with regard to the construction of bubble space around NH_4 in liquid NH_3. First, if the Rydberg space is totally repressed in liquid NH_3, the NH_4 radical is unstable.[11] The solvation energy of valence-like NH_4 and NH_3 (0.25 eV)[34] should be similar. In this case, reaction 6 will be exoergic. Secondly, if the bubble is created around the NH_4 unit, the $n > 0$ complexation energies will be lost. In this case, reaction 6 will be slightly exoergic because of the solvation energy of NH_3 (presumably 0 for H atom). Thirdly, if the bubble is constructed around the $NH_4(NH_3)_4$ structure by the repulsion of the NH_3 molecules external to this core, the 1.50-eV total complexation energy of the $NH_4(NH_3)_4$ is retained. If no solvation energy of this bubble is assumed, reaction 6 has to be modified: $(NH_4(NH_3)_4)_b = 5(NH_3)_s + H$. This reaction enthalpy can be estimated at +0.25 eV (i.e., $+1.50 - (5 \times 0.25)$, assuming no solvation energy for the H atom). One could consider $(NH_4(NH_3)_4)_b$ as the preferred bubble structure for NH_4 in liquid NH_3 or large clusters for the following reasons. At the $n = 5$, 6 level, the stepwise complexation energies have approached the solvation energy of NH_3. At this level there is no advantage in transfering NH_3 units from solvent to bubble. Therefore, the bubble should reach optimum size at $n = 4$. One could anticipate a stabilizing migration of the $NH_4(NH_3)_4$ bubble to the surface. This will allow using empty space above the surface for Rydberg occupation while still taking advantage of the $n = 5$, 6 complexation energy. Our computations (Table V) showed that proton transfer in the NH_4NH_3 radical complex (TS shown in Figure 7) has a sufficiently low barrier (0.2 eV) to permit either thermal or tunnel bubble migration. In this case bubble diffusion occurs by a hopping mechanism in which the hydrogen and Rydberg migration are coupled.

There is no definitive experimental proof for the existence of ammonium radicals in liquid NH_3. On electrolysis[5e] in liquid NH_3, tetraalkylammonium cations yield solvated electron spectra quantitatively indicating that the equilibrium constant, $(R_4N^+)_s + (e^-)_s = (R_4N)_s$, must lie well to the left. However, in the case of tetraalkylammonium radicals solvation will not be large. The solvated electron in liquid NH_3 is not indefinitely stable at −70 °C in the presence of fully alkylated quaternary salts. Reaction occurs, presumably $R_4N = R_3N + R$. However, this reaction does not require R_4N as a real intermediate. Electrolysis[35] of any quaternary salt having at least one NH bond results in immediate decomposition and release of H_2.

Kinetically, the reaction $(NH_4^+)_s + (e^-)_s$ has a rate constant, 10^6 M^{-1} s^{-1}, well below the diffusion-controlled limit.[5c,f] If NH_4 were present and much more stable than $(NH_4^+)_s + (e^-)_s$, one would have expected a diffusion-controlled rate for removal of the electron and some buildup of NH_4 radical. The decomposition of the NH_4 radical could then be partially bimolecular owing to the presumably rapid reaction[36] of two NH_4 radicals to give molecular $H_2 + 2NH_3$. In fact, the electron reaction follows first-order kinetics. In addition, Schindewolf[34] has estimated the enthalpy of the reaction, $(NH_4^+)_s + (e^-)_s = (NH_3)_s + H$, at +0.31 eV. Given our above estimate of the enthalpy of reaction 6 (+0.25 eV), reaction 7 has an exothermicity of only 0.06 eV. Even without making any reaction entropy estimates, this enthalpy estimate indicates that the NH_4 radical should be a measurable intermediate in the reaction of $(NH_4^+)_s$ with $(e^-)_s$.

Exploitation of the IP data shown in Figure 6 requires another approach. First of all, the solvation energies of NH_4^+ and the electron in liquid NH_3 are estimated[34] at 4.45 and 0.99 eV, respectively. Using the gas-phase IP of NH_4 (4.73 eV), the enthalpy for the following reaction can be estimated at −0.71 eV. In estimating the solvation energy for the NH_4 species

$$NH_4(g) = (NH_4^+)_s + (e^-)_s$$

we still assume $(NH_4(NH_3)_4)_b$ as the preferred structure of $(NH_4)_s$. The energy for the reaction, $NH_4(g) + 4(NH_3)_s = (NH_4(NH_3)_4)_b$, requires first removing four NH_3 molecules from liquid ammonia to the gas phase (4×0.25 eV = 1.00 eV), followed by forming $NH_4(NH_3)_4$ (−1.50 eV). Ignoring the cavitation energy,[37] and again assuming zero bubble solvation energy, the solvation energy, $NH_4(g) = (NH_4)_s$ is estimated at only −0.50 eV. In this case, the enthalpy of reaction 7 is −0.21 eV. This is in fortuitous agreement with the above estimate of −0.06 eV, especially given the larger uncertainties in the estimated NH_4^+ and electron solvation energies.

Figure 6 indicates that the cluster ionization potentials are much larger than the above reaction 7 estimates. Part of the discrepancy is due to the fact that Figure 6 does not take into account the solvation energy of the electron in liquid NH_3 (0.99 eV).[34] A better comparison can be made subtracting 0.99 eV from the IPs shown in Figure 6. This adjustment would still predict a liquid vertical IP of about 2 eV for the $(NH_4(NH_3)_4)_b$ bubble. What

(32) Kassab, E.; Evleth, E. M., to be published. This is a study of excited singlet and triplet NH_3 surrounded by large numbers of He atoms (up to 20) and H_2 molecules. Electron density maps show that, depending on the distance of the surrounded molecules, the Rydberg orbital adjusts to avoid these structures. There are nodal regions in the 3s orbital showing repulsive or antibonding relations with these structures.

(33) (a) Haberland, H.; Schlinder, H.-G.; Worsnop, D. R. *Ber. Bunsenges. Phys. Chem.* **1984**, *88*, 270–272. (b) Haberland, H.; Ludwigt, C.; Schlinder, H.-G.; Worsnop, D. R. *Surf. Sci.* **1985**, *156*, 157–164.

(34) (a) Schindewolf, U. *Ber. Bunsenges. Phys. Chem.* **1982**, *86*, 887–894. (b) Schindewolf, U. *J. Phys. Chem.* **1984**, *88*, 3820–3826.

(35) See references cited in footnote 5e.

(36) Kassab, E.; Fouquet, J.; Evleth, E. M., paper in preparation. Only an activation energy of several kcal/mol is found for the reaction: $2NH_4 = 2NH_3 + H_2$.

(37) Claverie, P.; Daudey, J. P.; Langlet, J.; Pullman, A.; Piazzola, D.; Huron, M. J. *J. Phys. Chem.* **1978**, *82*, 405–418.

is needed is an estimate of the cation complexation energy in going from $n = 4$ to $n = \infty$. The $n = 5$ and 6 calculations (Table IV) indicate that a single NH_3 solvation of each NH_3 on the $NH_4^+(NH_3)_4$ core will at least produce an $n = 4$ to $n = 8$ stabilization of 4×0.3 eV, or 1.2 eV. In this case the adiabatic ionization potential of $(NH_4(NH_3)_4)_b$ in liquid NH_3 (reaction 7) cannot be more than 0.8 eV. Further solvation of the cation will produce additional lowering.[36] This argument supports the above conclusion that in liquid ammonia the reaction $(NH_4)_s = (NH_4^+)_s + (e^-)_s$ is not far from being isoergic. However, none of these analyses can quantitatively establish the reaction enthalpies of reactions 6 and 7.

Conclusion

We have shown the theoretical origins of the stability of the isolated NH_4 radical. An analysis of its stability on NH_3 complexation for $n > 3$ is still not clear owing to the Rydberg character of this species. Extension of this analysis to liquid NH_3 is possible if one assumes a Rydberg $NH_4(NH_3)_4$ bubble structure. This final analysis indicates that NH_4 and $NH_4^+ + e^-$ are about isoergic in liquid ammonia even though the ionization potential of NH_4 is 4.7 eV in the gas phase. The final irony of this analysis is that NH_4 radical is predicted to have stability only in the form of intermediate-sized clusters. However, the species is anticipated to play a role in the chemical reactions in liquid ammonia.

Acknowledgment. All computations presented here were done at the CNRS Computing Center (CICRE) at Orsay, France. The authors thank the computing staff at this center for their aid.

Registry No. H_4N^+, 92075-50-8; $(CH_3)_4N^+$, 21265-91-8; NH_3, 7664-41-7.

Absolute Stereostructure of Novel Chiral Troponoid Spiro Compounds as Determined by Theoretical Calculation of CD Spectra

Nobuyuki Harada,*[1a] Hisashi Uda,[1a] Tetsuo Nozoe,[1b] Yoshio Okamoto,[1c] Hidetsugu Wakabayashi,[1d] and Sumio Ishikawa[1d]

Contribution from the Chemical Research Institute of Nonaqueous Solutions, Tohoku University, 2-1-1 Katahira, Sendai 980, Japan, the Tokyo Research Laboratories, Kao Corporation, 1-3 Bunka, Sumida, Tokyo 131, Japan, the Faculty of Engineering Science, Osaka University, Toyonaka, Osaka 560, Japan, and the Faculty of Science, Josai University, Sakado, Saitama 350-02, Japan. *Received September 29, 1986*

Abstract: The absolute stereostructures of the chiral troponoid spiro compounds, cyclohepta[1,2-*b*:1,7-*b'*]bis[1,4]benzoxazine (**1**) and cyclohepta[1,2-*b*:1,7-*b'*]bis[naphth[2,3-*e*][1,4]oxazine] (**2**), were determined by theoretical calculation of CD spectra. The spiro compounds with a C_2-symmetrical structure were optically resolved by means of HPLC using a chiral stationary phase of (+)-poly(triphenylmethyl methacrylate). The first-eluted enantiomer of compound **1** exhibits the very intense negative optical rotation $[\alpha]_D$ −4700° and strong CD Cotton effects, indicating that the conjugated π-electron system spread over the whole area of the molecule is strongly twisted. In order to determine the absolute configuration of the twisted π-electron system, the CD spectrum of (15a*S*)-**1** was calculated by application of the π-electron SCF–CI–dipole velocity MO method. The calculated CD and UV values are in good agreement with the observed data: calcd CD, λ_{ext} 394 nm, $\Delta\epsilon$ −106.9 and λ_{ext} 289 nm, $\Delta\epsilon$ +76.3; calcd UV, λ_{infl} 394 nm, ϵ 8000, λ_{max} 284 nm, ϵ 23 500; obsd CD, λ_{ext} 398 nm, $\Delta\epsilon$ −45.3 and λ_{ext} 287 nm, $\Delta\epsilon$ +80.4; obsd UV, λ_{max} 378 nm, ϵ 7900 and λ_{max} 285 nm, ϵ 23 500. Accordingly, the absolute configuration of (−)-**1** was theoretically determined to be 15a*S*. The present conclusion is in line with the X-ray crystallographic results. The absolute configuration of compound (−)-**2**, a spiro acetal with two naphthalene chromophores, was similarly determined to be 18a*S* by application of the same method: calcd CD, λ_{ext} 403 nm, $\Delta\epsilon$ −120.0, λ_{infl} 330 nm, $\Delta\epsilon$ +38.0, λ_{ext} 272 nm, $\Delta\epsilon$ +109.0; calcd UV, λ_{infl} 402 nm, ϵ 13 700, λ_{max} 316 nm, ϵ 22 200, λ_{max} 255 nm, ϵ 41 000; obsd CD, λ_{ext} 405 nm, $\Delta\epsilon$ −42.9, λ_{ext} 319 nm, $\Delta\epsilon$ +28.9, λ_{ext} 273 nm, $\Delta\epsilon$ +103.3; obsd UV, λ_{max} 390 nm, ϵ 11 500, λ_{max} 308 nm, ϵ 23 900, λ_{max} 262 nm, ϵ 39 100.

The CD exciton chirality method for determination of absolute configuration on the basis of a chiral exciton coupling mechanism has been extensively applied to various chiral natural and synthetic organic compounds.[2] The exciton method, however, is not always applicable to all kinds of organic compounds. For example, 1,8a-dihydro-3,8-dimethylazulene is one of such difficult cases, to which the CD exciton chirality method is not directly applied. For such a compound with a twisted conjugated π-electron system, the theoretical calculation of CD spectra by the π-electron SCF–CI–dipole velocity MO method[2-5] is useful for determination of absolute stereostructures. In fact, we have succeeded in determining the absolute stereochemistry of optically active 1,8a-dihydro-3,8-dimethylazulene, a natural product isolated from the cell culture of the liverwort *Calypogeia granulata* Inoue as a labile biosynthetic intermediate for 1,4-dimethylazulene, by the theoretical calculation of CD spectra.[6] The CD curve calculated for 1,8a-dihydroazulene with a twisted conjugated tetraene system was in a good agreement with the observed spectrum, leading to the unequivocal determination of absolute configuration.

In this report, we describe the determination of the absolute stereostructure of novel tropoquinoid spiro compounds **1** and **2** with a twisted conjugated π-electron system which is spread over the whole area of the molecules, by application of the π-electron

(1) (a) Tohoku University. (b) Kao Corp. (c) Osaka University. (d) Josai University.

(2) Harada, N.; Nakanishi, K. *Circular Dichroic Spectroscopy—Exciton Coupling in Organic Stereochemistry*; University Science Books: Mill Valley, Calif., and Oxford University Press: Oxford, 1983.

(3) Moscowitz, A. *Tetrahedron* **1961**, *13*, 48.

(4) Kemp. C. M.; Mason, S. F. *Tetrahedron* **1966**, *22*, 629. Brown, A.; Kemp, C. M.; Mason, S. F. *J. Chem. Soc. A* **1971**, 751.

(5) Harada, N.; Tamai, Y.; Takuma, Y.; Uda, H. *J. Am. Chem. Soc.* **1980**, *102*, 501. Harada, N.; Tamai, Y.; Uda, H. *Ibid.* **1980**, 102, 506.

(6) Harada, N.; Kohori, J.; Uda, H.; Nakanishi, K.; Takeda, R. *J. Am. Chem. Soc.* **1985**, *107*, 423.

0002-7863/87/1509-1661$01.50/0